ELSEVIER

Chemical Engineering Journal 71 (1998) 49–56

Chemical Engineering Journal

Lamellar modelling of reaction, diffusion and mixing in a two-dimensional flow

Michael J. Clifford[a,*], Stephen M. Cox[a], E.P.L Roberts[b]

[a] *Division of Theoretical Mechanics, School of Mathematical Sciences, University of Nottingham, University Park, Nottingham NG7 2RD, UK*
[b] *Department of Chemical Engineering, UMIST P.O. Box 88, Manchester M60 1QD, UK*

Received 7 December 1997; received in revised form 27 May 1998; accepted 16 June 1998

Abstract

We present a one-dimensional model of reaction, diffusion and mixing in a two-dimensional flow. The model assumes that initially segregated reactants are stretched and folded into a lamellar structure. Reaction and diffusion are simulated within this one-dimensional lamellar array. The lamellae are assumed to have a uniform thickness. Mixing is included as a single parameter i.e. the average stretch rate of the flow. Results are compared with full two-dimensional simulations of the concentration fields. Given the very simple nature of the one-dimensional model and the complexity of the full system, remarkably good agreement is obtained with a considerable saving in computational effort. For a competitive–consecutive reaction the predicted yields agree to within 6%. A typical one-dimensional simulation on a Silicon Graphics R5000 workstation takes around 1 min compared to 25 h on a 1024-node nCUBE 2 parallel computer for the concentration field simulations. The one-dimensional lamellar simulations are not limited by the relative rates of diffusion, reaction and advection, and are generally applicable to complex two-dimensional and, in principle, three-dimensional flows.

Keywords: Lamellar modelling; Lamellar structure; Two-dimensional flow

1. Introduction

Numerical simulation of chemical reactions in fluid flows is a problem that has been of interest to many researchers [1–4]. Two major goals of much of the research into such systems are: (i) predicting the rate of reaction, and (ii) determining the quality of the product – the ratio between desired products and waste, formed in secondary, simultaneous (and unwanted) reactions. Clearly these issues are important for industrial chemical reaction processes. In this paper, we address both issues for a two-stage reaction in a two-dimensional chaotic laminar flow. (Higher dimensional flows and turbulent modelling are beyond the scope of this work.)

In principle, if the velocity field is known, it is possible to simulate the development of the full concentration field for a given system. For systems where the rate of diffusion is relatively low, however, this approach becomes impractical. The fluid mixing can generate a very complex structure with small scale variations of the concentration field before significant diffusion can occur. In these circumstances a prohibitively large numerical grid is required to describe the concentration field.

Simulations of this kind have recently been carried out by Muzzio and Liu [3], hereafter referred to as ML, who examined the progress of the two-stage reaction $A+B\rightarrow R$, $B+R\rightarrow S$ in a chaotic fluid flow. In particular they were concerned with the relative yields of R and S, and the extent to which reactants were trapped inside islands within the chaotic fluid flow. However, the parameter regimes in which simulations can be carried out are restricted, and these simulations are computationally expensive.

The fluid flow generates a complicated pattern of striations of reactants. As time evolves, more and more, thinner and thinner striations are generated by the stretching and folding action of the flow. Diffusion of reactants is most rapid in the high concentration gradients of the thinnest striations, and these striations are rapidly smeared out, facilitating chemical reaction. Although the detailed picture is very involved, the formation of striations suggests that a relatively simple model may usefully be applied. In this model the complicated pattern of striations is replaced by one-dimensional array of lamellae, in which reaction and

*Corresponding author. Tel.: +44-115-9513848; fax: +44-115-951387; e-mail: mike.clifford@nottingham.ac.uk

1385-8947/98/$ – see front matter
PII: S1385-8947(98)00107-7

diffusion take place. Rather than repeating the two-dimensional simulations of ML, here our objective is to apply one-dimensional lamellar model to their system and to investigate quantitatively the utility of the model. The problem then becomes one of reactions and diffusion in a one-dimensional array, and yields a considerable saving of computational time. In addition, the lamellar model is not restricted to the parameter regimes of the full two-dimensional simulations.

Much work has been directed towards the analysis and numerical simulation of the single-step reaction A+B→R in a one-dimensional lamellar structure. Numerical simulations were first carried out by Muzzio and Ottino [5,6] and subsequently in a series of papers by Sokolov and Blumen [7–10] in the limit of infinitely fast reaction. In this event, there are well-defined lamellae because the reactants cannot coexist. When the reaction rate is finite and reactants are free to diffuse, the lamellar structure becomes progressively smeared out.

In all of these works the lamellar array is of fixed width, whereas we know that the action of the fluid stirring is to stretch regions of fluid and produce ever thinner striations. Such stretching may be accommodated within the lamellar model by placing the lamellae in a velocity field that causes the lamellar structure to become progressively thinner. The corresponding reaction–diffusion–advection equations may be reduced to a reaction–diffusion system [11,1] by applying a coordinate transformation. The choice of velocity field might reasonably be such that the width of the lamellar array decreases exponentially with time. Then the time taken for a lamellar width to halve is inversely proportional to the Lyapunov exponent (which is an average stretch rate) of the underlying two-dimensional velocity field.

In this paper, we carry out simulations of reaction, diffusion and advection using a one-dimensional lamellar model for a two-dimensional chaotic flow. The flow and parameter values are chosen to enable comparisons with the two-dimensional simulations of ML.

Comparison is made between the results from our one-dimensional simulations, and the 'full' two-dimensional simulations of ML.

2. The two-dimensional reaction–diffusion–advection problem

We consider the competitive-consecutive (or two-step) reaction

$$\mathrm{A} + \mathrm{B} \xrightarrow{k_1} \mathrm{R}, \quad \mathrm{B} + \mathrm{R} \xrightarrow{k_2} \mathrm{S} \tag{1}$$

where the rate constant for the production of R greatly exceeds that for S, i.e.

$$\frac{k_2}{k_1} = \epsilon \ll 1 \tag{2}$$

The reactants A and B are initially segregated and the products R (desired product) and S (unwanted by-product) are initially absent. The reactions take place in a fluid undergoing prescribed two-dimensional flow, $\mathbf{u}=(u, v)$.

We let c_A, c_B, c_R c_S denote the concentrations of the corresponding chemical species and suppose that the two-dimensional system may be described by the following coupled reaction–diffusion–advection system:

$$\frac{\partial c_\mathrm{A}}{\partial t} + \boldsymbol{u} \cdot \nabla c_\mathrm{A} = D\nabla^2 c_\mathrm{A} - k_1 c_\mathrm{A} c_\mathrm{B} \tag{3}$$

$$\frac{\partial c_\mathrm{B}}{\partial t} + \boldsymbol{u} \cdot \nabla c_\mathrm{B} = D\nabla^2 c_\mathrm{B} - k_1 c_\mathrm{A} c_\mathrm{B} - k_2 c_\mathrm{B} c_R \tag{4}$$

$$\frac{\partial c_\mathrm{R}}{\partial t} + \boldsymbol{u} \cdot \nabla c_\mathrm{R} = D\nabla^2 c_\mathrm{R} + k_1 c_\mathrm{A} c_\mathrm{B} - k_2 c_\mathrm{B} c_\mathrm{R} \tag{5}$$

$$\frac{\partial c_\mathrm{S}}{\partial t} + \boldsymbol{u} \cdot \nabla c_\mathrm{S} = D\nabla^2 c_\mathrm{S} + k_2 c_\mathrm{B} c_\mathrm{R}, \tag{6}$$

where t is time, D is the diffusivity (assumed to be the same for all chemical species) and ∇ is the two-dimensional differential operator $(\partial/\partial x, \partial/\partial y)$.

Following ML, we rescale the system of equations and make the problem dimensionless by setting

$$T = \frac{tU_0}{L_0}, \qquad \boldsymbol{X} = \frac{x}{L_0}, \qquad \boldsymbol{U} = \frac{\boldsymbol{u}}{U_0}. \tag{7}$$

Here U_0 is a typical velocity component of the fluid flow and L_0 is a typical length scale for the fluid domain. We non-dimensionalise the chemical concentrations, dividing each by $c_{\mathrm{B}0}$, the initial concentration of species B. The dimensionless system is then the reaction–diffusion–advection system

$$\frac{\partial \mathrm{A}}{\partial t} + \boldsymbol{U} \cdot \nabla \mathrm{A} = \frac{1}{\mathrm{Pe}}\nabla^2 \mathrm{A} - \frac{\mathscr{D}}{\mathrm{Pe}}\mathrm{AB} \tag{8}$$

$$\frac{\partial \mathrm{B}}{\partial T} + \boldsymbol{U} \cdot \nabla \mathrm{B} = \frac{1}{\mathrm{Pe}}\nabla^2 \mathrm{B} - \frac{\mathscr{D}}{\mathrm{Pe}}\mathrm{AB} - \frac{\epsilon\mathscr{D}}{\mathrm{Pe}}\mathrm{BR} \tag{9}$$

$$\frac{\partial \mathrm{R}}{\partial T} + \boldsymbol{U} \cdot \nabla \mathrm{R} = \frac{1}{\mathrm{Pe}}\nabla^2 \mathrm{R} + \frac{\mathscr{D}}{\mathrm{Pe}}\mathrm{AB} - \frac{\epsilon\mathscr{D}}{\mathrm{Pe}}\mathrm{BR} \tag{10}$$

$$\frac{\partial \mathrm{S}}{\partial T} + \boldsymbol{U} \cdot \nabla \mathrm{S} = \frac{1}{\mathrm{Pe}}\nabla^2 \mathrm{S} + \frac{\epsilon\mathscr{D}}{\mathrm{Pe}}\mathrm{BR} \tag{11}$$

where ∇ is now $(\partial/\partial X, \partial/\partial Y)$. This non-dimensionalisation introduces two new dimensionless parameters, the second Damköhler number,

$$\mathscr{D} = \frac{k_1 c_{B0} L_0^2}{D} \tag{12}$$

and the Péclet number,

$$\mathrm{Pe} = \frac{U_0 L_0}{D} \tag{13}$$

Pe is the ratio of the characteristic time for diffusion to that for advection, and is typically very large in many physical applications. In numerical simulations, a large Péclet number can generate computational difficulties as a fine numerical grid is required to resolve the large gradients in the concentration field that may arise. Since our simulations are

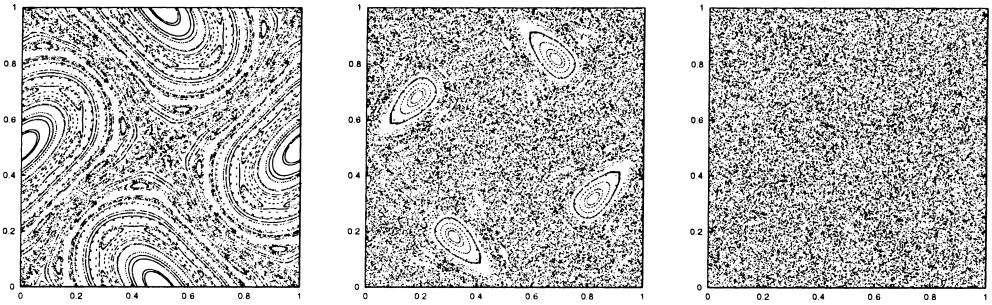

Fig. 1. Poincaré sections of the sine flow. The three cases are T_P=0.4, T_P=0.8 and T_P=1.6.

restricted to a single dimension, we require substantially fewer nodes than we would for equivalent simulations in two or three dimensions. Hence we can carry out simulations at larger Péclet number than would be possible in higher dimensions. To allow comparison with the results of ML we set Pe=10^4. The ratio $\Omega = \mathscr{D}/\mathrm{Pe}$ is the ratio of the characteristic time for advection to that for reaction. We examine three cases: $\mathscr{D}=10^3$ (Ω=0.1 slow reactions), $\mathscr{D}=10^4$ (Ω=1 intermediate), and $\mathscr{D}=10^5$ (Ω=10 fast reactions). However, real-life applications typically have Péclet numbers in the range from Pe=10^2 (laminar flames) to Pe=10^{10} or higher (turbulent reactive flows, polymerizations) [3].

2.1. The sine flow

Until recently, the complexity of the reaction–diffusion–advection problem has restricted numerical studies to one dimension. However, with the advent of parallel computers, ML were able to simulate mixing, diffusion and reaction for a simple two-dimensional model: the two-dimensional sine flow. While this flow may seem unrealistic, it can exhibit an extensive repertoire of mixing behaviours, and, as we shall see, data obtained from this system is useful for comparison with results from our one-dimensional simulations. This time-periodic flow is defined in the square domain $0\leq x\leq 1$, $0\leq y\leq 1$ by two motions:

$$u = \sin 2\pi y, \qquad v = 0, \quad \text{for } (n-1)\,T_P \leq t < (n-1/2)T_P \tag{14}$$

$$u = 0, \qquad v = \sin 2\pi x, \quad \text{for } (n-1/2)T_P \leq t < nT_P \tag{15}$$

where u and v are the x and y components of the velocity field, T_P is the period, and the integer n is the number of periods. The flow domain has periodic boundaries.

By varying the period, T_P a large range of mixing behaviours is possible. Following ML, we consider three cases: T_P=0.4, 0.8, 1.6. Poincaré sections obtained by plotting the position of several points after many periods are shown in Fig. 1. The first case, T_P=0.4, shows poor mixing. Two large islands form barriers to fluid transport, and any fluid contained inside an island can escape only by diffusion. However, the flow in the 'X' shaped region is chaotic, and mixing here is (locally) good. The second case, T_P=0.8, is shown in Fig. 1(b). Four small islands are present, covering around 20% of the flow domain. Smaller islets are also present. The final case, T_P=1.6, shown in Fig. 1(c) is essentially globally chaotic. Small islands do exist, but they occupy only a small proportion of the flow domain.

In order to quantify the mixing achieved in each case, we consider the mapping from a fluid particle's position (x_0, y_0) at time t=0 to its position (x_1, y_1) one period later. The Jacobian of this mapping is

$$J(x_0,y_0) = \begin{pmatrix} \dfrac{\partial x_1}{\partial x_0} & \dfrac{\partial x_1}{\partial y_0} \\ \dfrac{\partial y_1}{\partial x_0} & \dfrac{\partial y_1}{\partial y_0} \end{pmatrix} = \begin{pmatrix} 1 & T_p\pi\cos(2\pi y_0) \\ T_p\pi\cos(2\pi x_{1/2}) & 1 + T_p^2\pi^2\cos(2\pi x_{1/2})\cos(2\pi y_0) \end{pmatrix} \tag{16}$$

where

$$x_{1/2} = x_0 + \frac{T_P}{2}\sin(2\pi y_0) \tag{17}$$

The Jacobian of the nth iterate of the mapping is then simply

$$J_n(x_0,y_0) = J(x_n,y_n)J(x_{n-1},y_{n-1})\cdots J(x_0,y_0) \tag{18}$$

where (x_k,y_k) is the position of the fluid particle at time $t=kT_P$. The eigenvalues Λ_1, Λ_2 of this matrix provide an indication of the stretch experienced by the fluid particle initially at (x_0,y_0). We introduce the finite-time Lyapunov exponent

$$\sigma_n(x_0,y_0) = \frac{1}{nT_P}\log\max(|\Lambda_1|,|\Lambda_2|) \tag{19}$$

Fig. 2 shows $\sigma_n(x_0,y_0)$ for the three cases T_P=0.4, 0.8, 1.6 for n up to 500; in each case four different choices of initial position (x_0, y_0) are illustrated. The convergence of $\sigma_n(x_0, y_0)$ as n becomes large is slow. We define $\sigma_\infty = \lim_{n\to\infty}\sigma_n$ and estimate σ_∞=0.6, 0.8, 1.2 for T_P=0.4, 0.8, 1.6, respectively.

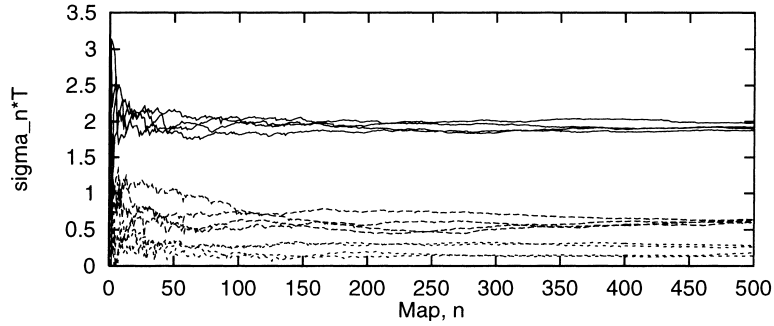

Fig. 2. Plot of $\sigma_n T_P$ against number of maps n for T_P=1.6 (solid lines), T_P=0.8 (dashed lines), T_P=0.4 (dotted lines).

The values of $\sigma_n(x_0, y_0)$ vary considerably with the choice of (x_0, y_0). This has implications for the one-dimensional model; since, as we shall see later, most of the reaction has taken place after 8 dimensionless time units, well before the asymptotic regime as $n\rightarrow\infty$ in which $\sigma_n(x_0, y_0)$ is independent of (x_0, y_0). This corresponds to n=20 for T_P=0.4, n=10 for T_P=0.8, and n=5 for T_P=1.6. Hence, individual fluid elements will experience a whole range of stretching rather than the uniform stretch we use in our one-dimensional lamellar model.

3. The lamellar model

As we have already mentioned, the (laminar) chaotic mixing of fluids creates evolving structures consisting of stretched and folded striations. The stretching is due to the divergence of neighbouring chaotic trajectories and leads to a thinning of the striations with time, whilst the folding is a global property which is necessary if the fluid is to remain in a finite domain. The stretching of the striations creates difficulties for the two-dimensional simulations since the numerical grid must be fine enough to describe the rapid changes in concentration across thin striations. However, the presence of these thin structures also suggests that the reaction and diffusion in the two-dimensional system may be modelled effectively by a one-dimensional array corresponding to taking a 'slice' across the striations. This assumption has been the foundation for many analytical and numerical studies [12,13,5,6].

Fig. 3 shows how a slice across a two-dimensional structure of striations can be utilised to provide input data for a one-dimensional lamellar model. The striations in Fig. 3(a) consist of alternating layers of chemical species A and B produced by mixing a blob of fluid B in a tank of fluid A, in the absence of reaction and diffusion. By taking a line roughly perpendicular to the striations and recording the concentrations of chemical species along the line, we generate segregated initial conditions for a one-dimensional simulation of reaction and diffusion (Fig. 3(b)). If diffusion and reaction are then allowed to take place in the one-dimensional lamellar structure, the reactant concentrations

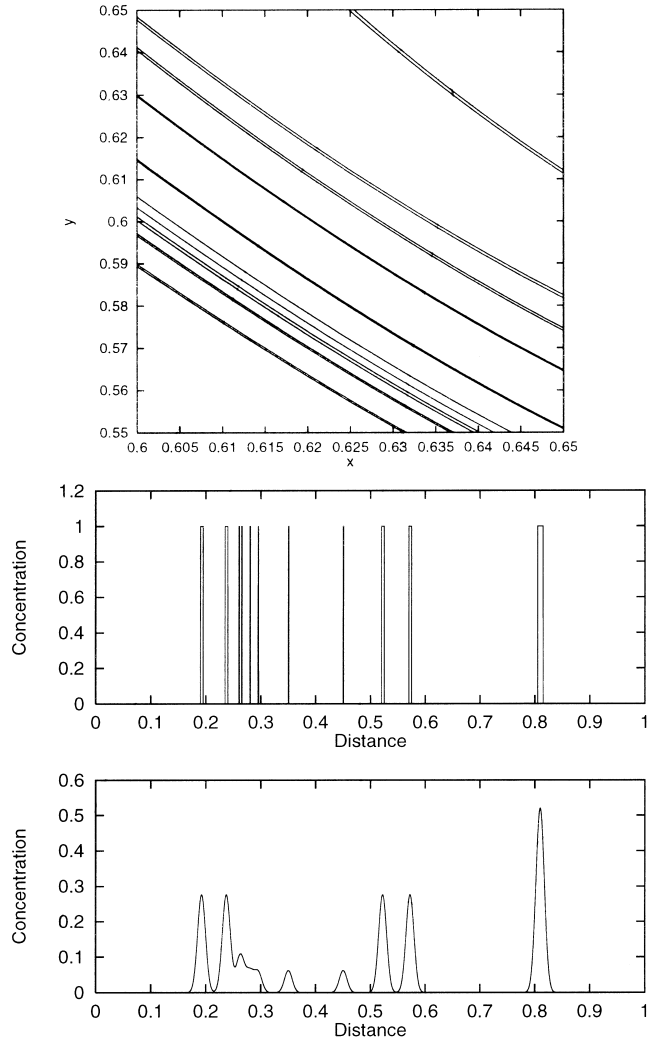

Fig. 3. (a) A close-up of a portion of the interface between chemical species A and B some time after a blob of B is placed in the sine flow. The velocity field stretches and folds the blob into a complicated structure consisting of many thin striations. (b) Concentration of B is plotted along a line cutting the striations. This concentration profile is taken as an initial state for a one-dimensional lammellar model. (c) The lammellae are allowed to diffuse and react in a one-dimensional array-concentration of species B is shown some time latter.

evolve in some fashion (see Fig. 3(c)) that blurs the boundaries of the lamellae.

Until recently, much of the one-dimensional analysis has concentrated on a somewhat artificial lamellar model where striations are produced initially by mixing without reaction or diffusion, and then reaction and diffusion are allowed to occur in the absence of further fluid mixing. However, fluid mixing can be incorporated into the one-dimensional model by placing the lamellae in a one-dimensional velocity field, $U=-\sigma_\infty X$, that causes the lamellar structure to become exponentially thinner with time [1,2,11]. The non-dimensional domain has width

$$L(T) = \exp(-\sigma_\infty T) \tag{20}$$

This exponential squashing of lamellae mimics the fluid mixing in the two-dimensional system. To describe the diffusion and reaction in the evolving lamellae, we rescale Eqs. (8)–(11) with the following scales for time and lengths: Pe, $L(T)$. As a consequence, the term $\boldsymbol{U}\cdot\nabla A$ is eliminated, and the dimensionless system is then the one-dimensional reaction–diffusion system

$$\frac{\partial \mathrm{A}}{\partial T} = \exp 2\alpha T \frac{\partial^2 \mathrm{A}}{\partial X^2} - \mathscr{D}\mathrm{AB} \tag{21}$$

$$\frac{\partial \mathrm{B}}{\partial T} = \exp 2\alpha T \frac{\partial^2 \mathrm{B}}{\partial X^2} - \mathscr{D}\mathrm{AB} - \epsilon\mathscr{D}\mathrm{BR} \tag{22}$$

$$\frac{\partial \mathrm{R}}{\partial T} = \exp 2\alpha T \frac{\partial^2 R}{\partial X^2} + \mathscr{D}\mathrm{AB} - \epsilon\mathscr{D}\mathrm{BR} \tag{23}$$

$$\frac{\partial \mathrm{S}}{\partial T} = \exp 2\alpha T \frac{\partial^2 S}{\partial X^2} + \epsilon\mathscr{D}\mathrm{BR} \tag{24}$$

We have retained the symbols for non-dimensional time, T, and space, X, coordinates, but no confusion should arise as from here on these terms refer to the one-dimensional reaction-diffusion system (Eqs. (21)–(24)). The stretching exponent $\alpha=\sigma_\infty \mathrm{Pe}$. We note that our rescaling of the width of the lamellar system by $L(T)$ has the effect of introducing a diffusion coefficient that increases exponentially with time while the reaction coefficient remains constant. In addition, the non-dimensional domain is now of *fixed* (unit) width. The exponential growth of the diffusion term comes as a consequence of keeping the non-dimensional domain at constant width. Rather than letting lamellae reduce in size, which would increase concentration gradients and thereby increase the rate of diffusion, we keep the width of the domain fixed so that the diffusion coefficient increases correspondingly with time.

The utility of this one-dimensional model is discussed in Section 4, where comparison is made with results from the two-dimensional reaction–diffusion–advection system.

3.1. Well-mixed reaction system

If the chemical species diffuse rapidly (with respect to the rate of chemical reaction), we consider the system to be homogeneous. This greatly simplifies the analysis; later when we discuss our numerical simulations we compare our results with a homogeneous system as a limiting case. Reaction in a well-mixed system has been described by [14,15]. One result used later is that the concentration of A can be determined as an implicit function of time from

$$T = \int_{A(T)}^{A_0} \frac{\mathrm{d}\alpha}{\alpha(1-2\mathrm{A}_0 + ((1-2\epsilon)/(1-\epsilon))\alpha + ((A_0^{1-\epsilon})/(1-\epsilon))\alpha^\epsilon)} \tag{25}$$

where $\mathrm{A}(0)=\mathrm{A}_0$, $\mathrm{B}(0)=1$, $\mathrm{R}(0)=0$, $\mathrm{S}(0)=0$.

4. Numerical simulations of the one-dimensional reaction–diffusion system

We have carried out numerical simulations of the one-dimensional reaction–diffusion system Eqs. (21)–(24) in the interval

$$0 \le X \le 1 \tag{26}$$

which initially contains a pair of lamellae of equal width, one of species A and one of species B.

Periodic boundary conditions are applied to the system, so that $\mathrm{A}(X+1, T)=\mathrm{A}(X, T)$ for all $T \ge 0$, and similarly for B, R, and S; thus a periodic array of lamellae is simulated.

The one-dimensional reaction–diffusion system is solved numerically using the method of lines [16]. A central difference operator is used to discretise the Laplacian operator, which reduces the problem to a system of coupled ordinary differential equations for the concentrations at the various spatial nodes. A NAG Library routine that implements a Runge–Kutta–Merson scheme is used to integrate the system forwards in time. The number of spatial nodes is taken to be 100, which provides more than adequate resolution.

4.1. Scope for mixing to affect the rate of reaction

Before we consider specific cases of mixing, diffusion, and reaction in a one-dimensional array, we investigate the extent to which fluid mixing could influence the reaction kinematics. If mixing is rapid (compared to reaction), then the rate of reaction will approach that of the well-mixed case, for which we have an analytical solution. On the other hand, if mixing is slow, then the lamellae will be squashed very slowly on average, and the rate of reaction will approach that of an initially segregated system with no squash ($\alpha=0$). Numerical results were obtained for $\Omega=0.1$, 1.0 and 10 with no squashing starting with a periodic array of lamellae (as above). Initially we set $\epsilon=0$, and ignore the secondary unwanted B+R→S reaction. The initial concentrations are $\mathrm{A}(X, 0)=1$, $\mathrm{B}(X, 0)=0$ for $0 \le X<0.5$, $\mathrm{A}(X, 0)=0$, $\mathrm{B}(X, 0)=1$ for $0.5 \le X<1$. The results are displayed in Fig. 4, where we plot the mean concentration of species A against time together with the results from the corresponding well-mixed reaction obtained from Eq. (25).

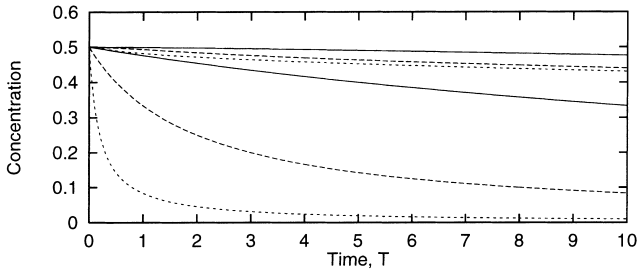

Fig. 4. Plot of the mean concentration of A against time. Upper three curves are for no mixing (α=0), and lower three curves are for well-mixed cases Ω=0.1 (solid line), Ω=1 (dashed line), and Ω=10 (dotted line). In each case the equations Eqs. (21)–(24) are solved numerically, subject to initially segregated or well-mixed initial distributions of species A and B.

We expect the results for one-dimensional simulations in exponentially shrinking physical domains to lie between the corresponding curves for the well-mixed and α=0 systems.

As can be seen clearly in the figure, the rate of reaction at early time depends crucially on the amount of mixing. This is in agreement with asymptotic predictions of the initial decay of reactants in two limiting cases: for systems with α=0, $A(0)-A(t) \propto t^{3/2}$ at early times, whilst $A(0)-A(t) \propto t$ for the well-mixed case [17]. The gap between the well-mixed and initially segregated curves widens as the Damköhler number increases.

4.2. One-dimensional reaction–diffusion simulations

One-dimensional simulations of Eqs. (21)–(24) were carried out in a periodic array of lamellae. Each flow is characterised using a stretch rate equal to the Lyapunov exponent. Three values of the Lyapunov exponent (σ_∞=0.6, 0.8, 1.2) corresponding to the simulations of the sine flow in Section 3 were used, each at Ω=0.1, 1 and 10. The results are displayed in Fig. 5, which should be compared with Fig. 8(a) of ML. We also include corresponding results for the two-dimensional simulations at Ω=1, carried out by ML. Our one-dimensional results are remarkably similar to the two-dimensional simulation results obtained by ML, the largest discrepancies being for slow mixing (T_P=0.4) at Ω=1, 10 which could be accounted for by the presence of islands in the two-dimensional flow. We note that the main differences between the one-dimensional and two-dimensional numerical simulations occur at early time – the early concentration of the reactant A falls much more rapidly in the two-dimensional case than in our one-dimensional simulations. To explain this phenomenon, we consider the interface between the reactants A and B in the two-dimensional flow in the absence of reaction and diffusion. In Fig. 6, we plot the growth rate of the interface,

$$\lambda = \frac{1}{t}\log\left(\frac{L_I(t)}{L_I(0)}\right)$$

against time. In our one-dimensional model, we assume that the length of the interface, $L_I(t)$, grows exponentially

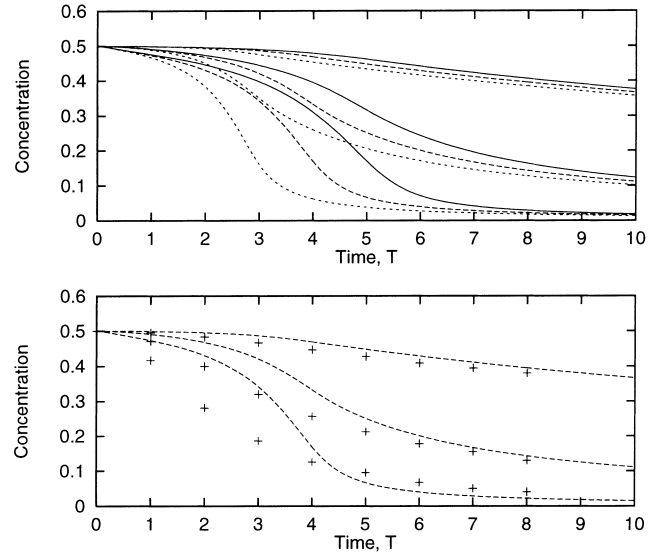

Fig. 5. Mean concentration of species A versus time. Upper figure: T_P=0.4 (solid lines), T_P=0.8 (dashed lines), and T_P=1.6 (dotted lines). Ω=0.1 (top three curves) Ω=1 (middle three curves), and Ω=10 (bottom three curves). The results from ML's two-dimensional simulations are compared with our one-dimensional results for T_P=0.8 in the lower figure.

according to the Lyapunov exponent: $L_I(t)=L_I(0)\exp(\sigma_\infty t)$. The predicted growth rates, λ=0.8, 1.3, and 1.5 should therefore be compared with the Lyapunov exponents, σ_∞=0.6, 0.8, and 1.2 for T_P=0.4, 0.8, and 1.6, respectively (determined in Section 2). We note that the interface grows faster than the Lyapunov exponent predicts in all cases. Hence, our one-dimensional simulations underestimate the fluid mixing that occurs in the two-dimensional flow at early times. This phenomenon has also been observed by Sawyers et al. [18].

4.3. Two-stage reaction

Whilst mixing affects the rate of reaction for the single-stage reaction, the eventual composition of the products relies solely on the initial concentrations of the chemical species A and B. However, for ϵ>0 in the competitive–

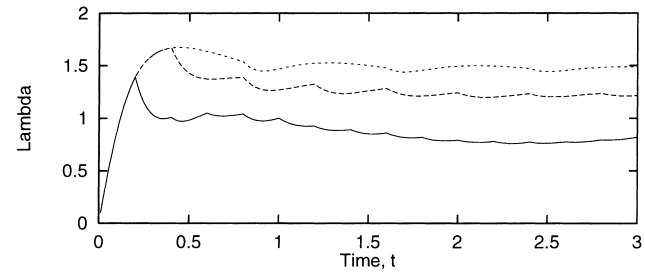

Fig. 6. Growth rate of the interface for T_P=0.4 (solid line), T_P=0.8 (dashed line), and T_P=1.6 (dotted line) against time. The asymptotic values λ=0.8, 1.3 and 1.5 should be compared to the Lyapunov exponents (0.6, 0.8, 1.2).

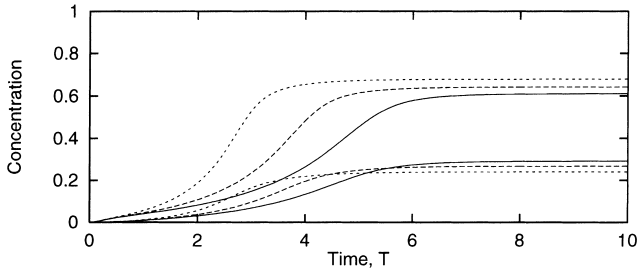

Fig. 7. Plots of $2\bar{R}(T)$ and $3\bar{S}(T)$, where $\bar{R}$ and $\bar{S}$ are the mean concentrations of species R (top 3 curves) and S (lower 3 curves). T_P=0.4 (solid lines), T_P=0.8 (dashed lines), and T_P=1.6 (dotted lines).

consecutive reactions (Eq. (1)), mixing affects both the rate of formation and the composition of the products R and S. Following ML, we set $\epsilon\mathscr{D} = 10^4$, and plot the mean concentrations of species R and S in Figs. 7 and 8. This figure should be compared with Fig. 11(b) of ML. In their two-dimensional simulations, ML set $\mathscr{D} = \infty$ to simplify the computational steps. This is unnecessary in our case, and instead we keep ϵ=0.1, and $\mathscr{D} = 10^5$. To quantify the utility of the one-dimensional model, we compare in Table 1 the final concentrations of the products R and S predicted by the one-dimensional simulations to the values obtained by ML's two-dimensional simulations. At a glance, the accuracy of the one-dimensional model is good, with concentrations of the desired product R within 6% of the two-dimensional

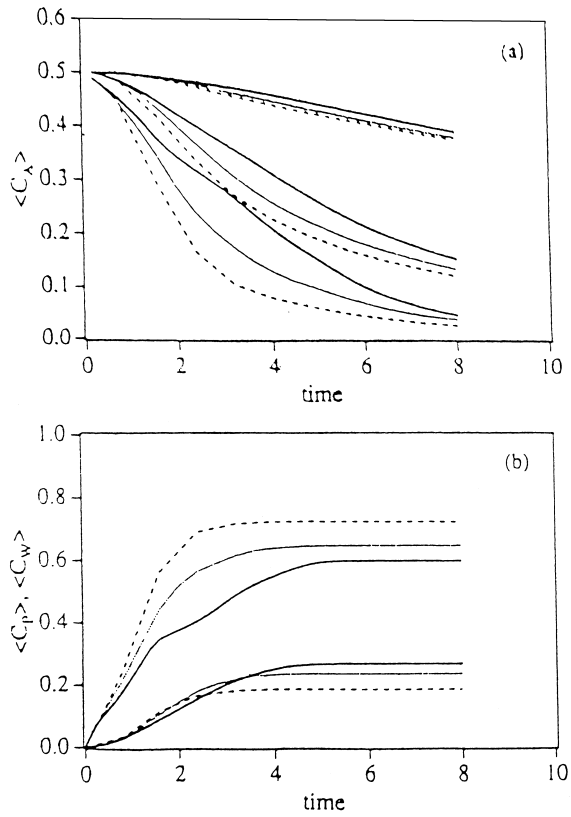

Fig. 8. Figures 8a, 11b from ML.

Table 1
Comparision between the final concentrations of the products R and S from the one-dimensional (R_{1D}, S_{1D}) and two-dimensional (R_{2D}, S_{2D}) numerical simulations

Mixing intensity	σ_∞	R_{1D}/R_{2D}	S_{1D}/S_{2D}
Low	0.6	102.8%	108.9%
Moderate	0.8	100.6%	113.0%
High	1.2	94.6%	129.3%

results. However, we note that the one-dimensional model predicts that for low and moderate mixing, more R will be formed than for the two-dimensional case. We can explain this over-estimate by the presence of large periodic islands in the low mixing case, and smaller islands in the moderate case (see Fig. 1). These islands reduce the amount of fluid mixing in the two-dimensional simulations, but are not taken into account by our simple one-dimensional simulations. It might be possible to develop a more sophisticated model by applying Eqs. (21)–(24) only to that part of the two-dimensional flow domain that experiences chaotic mixing, and by considering mixing in the islands separately. Although such an approach might provide a more realistic estimate of the final concentrations of the products, it is beyond the scope of this paper. Perhaps the most valuable estimate of the utility of the one-dimensional model is obtained by considering the results at high mixing. Here there are no periodic islands(at least, none of significant area) to affect the results. The discrepancies in this case (5.4% for R and 29.3% for S) are consistent with the growth of the interface exceeding that predicted by the Lyapunov exponent (see Fig. 6).

5. Discussion

We have demonstrated that the one-dimensional lamellar model is a useful tool in evaluating the products of diffusion, reaction and mixing in a two-dimensional system. The close agreement between reaction rates and also product quality for an albeit simple competitive–consecutive reaction scheme shows that the lamellar modelling approach followed by many researchers is justified. However, we need to extend these preliminary results to look at more complex reaction schemes and also to consider more realistic fluid flows as data becomes available.

Clearly the one-dimensional approach ignores important features in higher-order systems such as periodic islands, which need more careful consideration. However, if we are concerned with simulating reactions in chemical engineering applications we expect hindrances to mixing (such as periodic islands) to be removed by simple imposed perturbations, or other techniques. Reactor design should concentrate on generating a uniformly chaotic flow field to ensure uniform mixing, and this is coincidentally where the one-dimensional model is of most use. Hence we expect the

one-dimensional approach to be of particular interest to 'real-life' engineering applications. However, it remains to be seen if the model can reproduce more demanding experiments at higher Péclet number, with three-dimensional flow or with more complicated chemical kinetics. The simplicity of the model – we require only one parameter, namely, the Lyapunov exponent – makes it of use where the flow field is inaccessible, but the Lyapunov exponent can be measured by time-series analysis, for example. Using an exponent which measures the increase in intermaterial area would provide a better estimate for the mean squash.

The major weakness of the one-dimensional approach is that at early times where there are no lamellae as such, just a blob of fluid, the reaction and diffusion cannot be predicted accurately. The detailed behaviour of the system must then be obtained by consideration of the full two-dimensional model. (At early times it may be possible to follow the motion of the interface without the need for a prohibitively fine numerical grid.) A further limitation of the model comes from its use of a mean striation thickness. Realistic flows generate striations with widths spanning many orders of magnitude. Since the amount of waste produced at each location depends strongly on the local striation thickness, an estimate of the waste based solely on the mean thickness will almost always be an underestimate.

As a guide to the computational savings produced by using a one-dimensional model, each numerical simulation reported in this paper took less than 1 min to run on a Silicon Graphics R5000 Workstation whereas the two-dimensional calculations performed by ML each consumed about 25 h in a 1024-node nCUBE 2 parallel computer.

In conclusion, the simple one-dimensional model we have developed is a useful tool in estimating the yield from chemical reactions occurring in chaotic fluid flows. However, it has several important limitations, and hence should not be regarded as a replacement for higher dimensional models. Extensions to this work are currently in progress, and include attempting to predict the local concentration field from the one-dimensional model.

References

[1] J.M. Ottino, The kinematics of mixing: Stretching, chaos, and transport, Cambridge University Press, 1989.
[2] J. Baldyga, J.R. Bourne, A fluid mechanical approach to turbulent mixing and chemical reaction Part III. Computational and experimental results for the new micromixing model, Chem. Eng. Commun. 28 (1984) 259–281.
[3] F.J. Muzzio, M. Liu, Chemical reactions in chaotic flows, Chem. Eng. J. 64 (1996) 117–127.
[4] M.J. Clifford, E.P.L. Roberts, S.M. Cox, The influence of segregation on the yield for a series–parallel reaction, Chem. Eng. Sci. 53 (1998) 1791–1801.
[5] F.J. Muzzio, J.M. Ottino, Dynamics of a lamellar system with diffusion and reaction: Scaling analysis and global kinetics, Phys. Rev. A 40 (1989) 7182–7192.
[6] F.J. Muzzio, J.M. Ottino, Diffusion and reaction in a lamellar system: Self-similarity with finite rates of reaction, Phys. Rev. A 42 (1990) 5873–5884.
[7] I.M. Sokolov, A. Blumen, Diffusion-controlled reactions in lamellar systems, Phys. Rev. A 43 (1991) 2714–2719.
[8] I.M. Sokolov, A. Blumen, Reactions in systems with mixing, J. Phys. A: Math. Gen. 24 (1991) 3687–3700.
[9] I.M. Sokolov, A. Blumen, Distribution of striation thicknesses in reacting lamellar systems, Phys. Rev. A 43 (1991) 6545–6549.
[10] I.M. Sokolov, A. Blumen, Diffusion-controlled reactions in non-stoichiometrical layered systems, Physica A 191 (1997) 177–181.
[11] I.M. Sokolov, A. Blumen, Mixing effects in the A+B→0 reaction–diffusion scheme, Phys. Rev. Lett. 66 (1991) 1942–1945.
[12] L. Gálfi, Z. Rácz, Properties of the reaction front in an A+B→C type reaction–diffusion process, Phys. Rev. A 38 (1988) 3151–3154.
[13] H. Taitelbaum, B. Vilensky, A. Lin, A. Yen, Y.-E.L. Koo, R. Kopelman, Competing reactions with initially separated components, Phys. Rev. Lett. 77 (1996) 1640–1643.
[14] O. Levenspiel, Chemical Reaction Engineering, 2nd ed., Wiley, New York, 1972.
[15] N.M. Emanuel, D.G. Knorre, Chemical Kinetics, Wiley, 1973.
[16] W.F. Ames, Numerical Methods for Partial Differential Equations, 2nd ed., Academic Press, 1977.
[17] S.M. Cox, M.J. Clifford, E.P.L. Roberts, A two-stage reaction with initially separated reactants, Physica A 256 (1998) 65–86.
[18] D.R. Sawyers, M. Sen, H-C. Chang, Effect of chaotic interfacial stretching on biomolecular chemical reaction in helical-coil reactors, Chem. Eng. J. 64 (1996) 129–139.